Published in final edited form as:
Colloids Surf B Biointerfaces. 2013 February 1; 102: 111–116. doi:10.1016/j.colsurfb.2012.07.044.

Cell interaction study method using novel 3D silica nanoneedle gradient arrays

Deepak Rajput[a], **Spencer Crowder**[b], **Lucas Hofmeister**[c], **Lino Costa**[d], **Hak-Joon Sung**[e], and **William Hofmeister**[f,*]

[a]Center for Laser Applications, University of Tennessee Space Institute, Tullahoma, TN

[b]Department of Biomedical Engineering, Vanderbilt School of Engineering, Nashville, TN

[c]Department of Biomedical Engineering, Vanderbilt School of Engineering, Nashville, TN

[d]Center for Laser Applications, University of Tennessee Space Institute, Tullahoma, TN

[e]Department of Biomedical Engineering, Vanderbilt School of Engineering, AND Department of Medicine - Cardiovascular Medicine, Vanderbilt School of Medicine, Nashville, TN

[f]Center for Laser Applications, University of Tennessee Space Institute, Tullahoma, TN

Abstract

Understanding cellular interactions with culture substrate features is important to advance cell biology and regenerative medicine. When surface topographical features are considerably larger in vertical dimension and are spaced at least one cell dimension apart, the features act as 3D physical barriers that can guide cell adhesion, thereby altering cell behavior. In the present study, we investigated competitive interactions of cells with neighboring cells and matrix using a novel nanoneedle gradient array. A gradient array of nanoholes was patterned at the surface of fused silica by single-pulse femtosecond laser machining. A negative replica of the pattern was extracted by nanoimprinting with a thin film of polymer. Silica was deposited on top of the polymer replica to form silica nanoneedles. NIH 3T3 fibroblasts were cultured on silica nanoneedles and their behavior was studied and compared with those cultured on a flat silica surface. The presence of silica nanoneedles was found to enhance the adhesion of fibroblasts while maintaining cell viability. The anisotropy in the arrangement of silica nanoneedles was found to affect the morphology and spreading of fibroblasts. Additionally, variations in nanoneedle spacing regulated cell-matrix and cell-cell interactions, effectively preventing cell aggregation in areas of tightly-packed nanoneedles. This proof-of-concept study provides a reproducible means for controlling competitive cell adhesion events and offers a novel system whose properties can be manipulated to intimately control cell behavior.

Keywords

Cell-cell interactions; silica; femtosecond laser; nanoimprinting; nanofabrication; fibroblasts

*hof@utsi.edu.

Introduction

Studying a regulatory role of extracellular matrix (ECM) in cell behavior remains a key research area in developmental biology, biomedical engineering, and pharmacology [1, 2]. Cells sense physical and chemical signals arising from surface features (e.g., topography, compliance, texture, and anisotropy) of ECM and synthetic culture substrates, resulting in changes of their morphology, transcriptional behavior, and/or motility that are responsible for developmental processes and wound healing [3–6]. Hence, it is essential to understand the characteristic interaction between cells and specific surface features to further advance cell biology and regenerative medicine.

Since the effect of substrate topography on cell behavior was first studied with development of cell culture apparatus in 1890–1910's [7, 8], topographical control of cell behavior has been the subject of numerous review articles over the years [2, 3, 5, 6, 9–13]. The topographical features that have been studied range from unrefined patterns (e.g., grooves and ridges) [7, 8, 14–17] to precise topographical patterns and geometric profiles that are generated by photo or electron beam lithography [13, 18–20]. Recent studies on topographical control of cell behavior have been mostly done on 2D substrates in which the size of topographical features usually ranges from 10 nm to 3 μm [3] in an array form of nanogratings, nanopillars, or nanoholes [12, 21]. When these features are considerably larger in vertical dimension and are spaced at least one cell dimension apart, the features act as 3D physical barriers that specifically influence cell morphology, spreading, and alignment by guiding cell-matrix interaction ("contact guidance"), particularly observed in the case of fibroblast attachment and motility [22–25]. The contact guidance is mediated by an integrin-ligand interaction [26], resulting in alternation of cell attachment, orientation, viability, and motility [3, 15].

Three types of biomaterials (i.e., metals, ceramics, and polymers) are used for cell culture studies [3, 5, 9]. In particular, polymers are considered an efficient template to generate nano/microscale patterns via soft lithography. For example, micropillar arrays of polydimethylsiloxane (PDMS) and silicon prepared via lithographic techniques are used to study cellular responses to 3D microenvironments [9, 22, 25, 27]. Thermal properties of polymers can also be used to produce micro- and nanoscale features, which influence cellular behavior [28].

In this study, we investigated the physical behavior of NIH 3T3 mouse embryonic fibroblasts on an array of patterned silica nanoneedles. We used a recently-developed nanomachining technique whose biological application has not been explored yet. The pattern was a spatial 2D gradient array wherein needle spacing was varied from 10 μm to 50 μm in one micron increments (spacing = 10,11,12…50, 49, 48…10 μm) in both orthogonal directions. First, an array of nanoscale diameter holes (*nanoholes*) with 2D gradient spacing was prepared at the surface of fused silica by focusing single-pulses from an amplified femtosecond laser system using a high numerical aperture (NA) microscope objective lens (Figure 1). The fused silica template was etched to remove damaged material and slightly enlarge the nanoholes. A negative replica of the template was extracted with cellulose acetate (CA) by molding a CA film into the pattern creating an array of standing CA nanoneedles (Figure 2). A thin layer of silica was then deposited on CA nanoneedles by a low temperature chemical vapor deposition (CVD) process to form silica nanoneedles. This nanofabrication technique enables high resolution control of geometrical structures in a use-specified manner. NIH 3T3 fibroblasts were cultured on silica nanoneedles and their cell-cell and cell-matrix interactions were compared with those cultured on a flat silica surface prepared by the same CVD process. This proof-of-concept study provides a new gradient template method for controlling cell adhesion and function.

1. Materials and Methods

Nanoeedle Array Preparation

An amplified femtosecond laser system was operated in single-pulse mode to pattern fused silica substrate of 500 μm thickness in air using a 160× microscope objective lens (*NA* = 1.25 in water) with 780 nm laser pulse central wavelength, 160 fs temporal length, and ~5.2 μJ energy per pulse [29–31]. The pattern made on the template was a 2×2 matrix of quadrants, where each quadrant is a 2D gradient in nanohole spacing. In each quadrant, the spacing between the successive nanoholes, in both x and y directions, was first increased from 10 μm to 50 μm in 1 μm increments, and then reduced from 50 μm to 10 μm in 1 μm decrements, thus forming a 2D gradient in nanohole spacing. A schematic of the pattern (at reduced scale) is shown in Figure 1. The template was subjected to chemical etching in buffered oxide etch (Lodyne™, BOE, 6:1) for 30 seconds followed by rinsing in DI water, and then neutralized in 10M KOH for 3 minutes followed by rinsing in DI water (all at room temperature) prior to further use. Etching the template in BOE preferentially attacks laser affected regions in fused silica and widens the entrance of nanoholes. The depth of the nanoholes was determined to be at least 14 μm by cellulose acetate replication. The average entrance diameter was 750 nm post-etching.

A small piece of 35 μm thick cellulose acetate film was molded into the pattern using acetone solvent as shown in Figure 2A. After a few hours the resulting film was peeled off from the template using a pair of tweezers to remove the negative replica, a patterned array of cellulose acetate nanoneedles. The replica film was then glued to a 170 μm glass coverslip using a thin layer of uncured base PDMS (Sylgard® 184, Dow Corning Corporation) as an adhesive. CA replica-on-PDMS-on-glass coverslip was then left at room temperature for 24 hours for PDMS to crosslink for easy handling of the CA nanoneedles. The glass coverslip with CA replica was then placed on an aluminum SEM peg using a sticky tab (Lift-N-Press™, Structure Probe Inc., West Chester, PA) and subjected to a two-step chemical vapor deposition process at 65°C for silica deposition to form silica nanoneedles, details of which can be found in reference [29]. Briefly, CA replica was first exposed to silicon tetrachloride ($SiCl_4$) vapor for 5 minutes in a beaker and then to water vapor (H_2O) for 5 minutes in another beaker. Silicon tetrachloride molecules adsorbed at the surface of CA nanoneedles in the first beaker hydrolyze in the second beaker ($SiCl_4 + 2H_2O \rightarrow SiO_2 + 4HCl$) to form atop a thin silica coating of thickness 240 ± 40 nm. Silica nanoneedles thus formed are shown in Figure 2B–C and were used as a cell culture substrate. Flat silica substrates were prepared with unpatterned glass coverslip as a template using the same method (CA cast attached to glass with PDMS, followed by chemical vapor deposition).

Cell Experiments

NIH 3T3 fibroblasts were maintained in Dulbecco's Modified Eagle's Medium (DMEM, Gibco Cell Culture, Invitrogen, Carlsbad, CA, USA) supplemented with 10% heat-inactivated fetal bovine serum (FBS, Gibco) with 1% penicillin-streptomycin (P/S, Gibco) on tissue culture polystyrene in a water jacketed incubator at 37°C and 5% CO_2. For experiments, cells were seeded at a density of 80,000 cells / cm^2 and cultured either overnight or for three days for attachment/viability or immunocytochemistry experiments, respectively. For attachment and viability experiments, cells were treated with 4 μM Calcein AM (Molecular Probes, Invitrogen) in phosphate buffered saline (PBS, Gibco) for 15 minutes at 37°C. For immunocytochemistry, cells were fixed with 4% paraformaldehyde for 15 minutes, permeabilized with 0.25% Triton X in PBS for 10 minutes, and blocked with 10% goat serum in PBS. Unless otherwise stated, all steps were performed at room temperature. Cells were then incubated with phalloidin (Molecular Probes) for 20 minutes or

1:100 rabbit anti-mouse α smooth muscle actin primary antibody (αSMA, Abcam, Cambridge, MA) overnight at 4°C, followed by treatment of 1:50 FITC-conjugated goat anti-rabbit secondary antibody (Abcam) for 2 hours. Cells were imaged using a Nikon Eclipse Ti inverted fluorescence microscope (Nikon Instruments, Inc, Melville, NY). Images were analyzed with Image J (National Institutes of Health, Bethesda, MD) and n ≥50 cells from n ≥5 images were used for quantification. Individual cells, not those in aggregates, were quantified for shape descriptors (i.e., average cell area and average cell perimeter).

2. Results and Discussion

Cellular Response to Nanoneedles

The cellular response was altered in the presence of SiO_2 nanoneedles as compared to flat SiO_2 surfaces (Figure 3). Most strikingly, cell adhesion to surfaces with nanoneedles was an order of magnitude higher than adhesion to flat surfaces ($p = 0.005$, Figure 3A), while viability was maintained for cells adhered to either surface (Figure 3B). Cell spreading was also influenced by the presence of nanoneedles. On nanoneedle-containing surfaces, cells exhibited a larger area and perimeter than those cultured on flat surfaces ($p < 0.005$ and $p = 0.007$, Figure 3C and 3D, respectively), indicating increased cell spreading on the nanoneedle-containing surfaces. Therefore, the nanoneedle-containing surfaces were proven to promote cell-matrix interaction.

As seen in Figure 4, the presence and spacing of nanoneedles strongly influenced competitive cell-cell versus cell-matrix interactions. On flat substrates without nanoneedles, a significant number of cells formed large multicellular aggregates (Figure 4A; calcein, green) that did not display any noticeable organization or regularity (Figure 4B; αSMA, green; Hoechst, blue). In contrast, the presence of nanoneedles prevented cell aggregation, interrupted cell-cell contacts, and promoted interactions with the matrix (Figure 4C–F; αSMA, green; Hoechst, blue; actin, red). Cells preferentially aligned themselves along tightly spaced nanoneedles in gradient regions with sparse spacing in the orthogonal direction. In regions with sparse distributions in both directions, cells interacted both with adjacent nanoneedles as well as those located in the parallel rows (Figure 4C–D). In general, parallel rows of nanoneedles with substantial spacing between them (i.e. >30 μm) sequestered cells and biased them towards cell-matrix interactions. This spacing also controlled the size and geometry of any small cell clusters that were present (Figure 4E). A critical spacing between nanoneedles appeared to exist that regulated the ability of cells to adhere and spread in two dimensions (Figure 4F).

Relative spacing ratios for local regions of nanoneedles regulated cell spreading. Sparse spacing in two dimensions allowed single cells to spread in two dimensions (Figure 4C, top left inset), whereas tight spacing in one dimension and wide spacing in the orthogonal direction allowed cells to spread only in one direction (Figure 4C, top right inset). Given that nanoneedle spacing allowed for cells to attach between parallel rows, cells tended to spread in one dimension when the ratio between nanoneedles spacing in orthogonal directions was less than 0.5. In contrast, cells spread in two dimensions when nanoneedles spacing ratio was greater than 0.5. These data indicate that the cells actively sensed the microenvironment and that nanoneedle spacing can be used as a critical parameter to intricately regulate cell-cell and cell-matrix interactions.

In this study, we have employed a novel surface of patterened silica nanoneedles as a synthetic cell culture substrate and evaluated how needle presence and spacing affects cell attachment, morphology, and alignment. The impact of this work lies in the translation of a new material fabrication technique whose application to biology allows for the design of culture substrates that direct and regulate cell behavior. Specifically, the cellular response to

silica nanoneedles provides a means to directly modulate competitive cell adhesion events. Competitive cell-cell and cell-matrix interactions are a fundamental regulator of embryogenesis [11] and have been manipulated for complex tissue engineering strategies [32]. Cells of different lineages exhibit biased interactions depending upon their physiological location and function. For example, sheet-like epithelial and endothelial cells are dominated by cell-cell contacts through which various signals can be propagated, yet cells of a mesenchymal lineage are primarily cell-matrix interactive. Intricate lineage transition events, such as mesenchymal-to-epithelial transition (MET) and its reverse (EMT), confer new characteristics to differentiated cells that can also involve pathological progression. In certain cancers, for example, malignant cells in a primary tumor can undergo such a lineage transition, allowing them to escape from their normal location and metastasize [33]. By probing and modulating cell adhesion events, fundamental processes involved in embryogenesis, tissue engineering, and cancerous transformation can be intimately controlled, studied, and exploited for therapeutic intervention.

Fibroblasts, a mesenchymal cell type, are involved in diverse body processes including normal wound healing and pathological fibrosis. In healthy wound healing, fibroblasts express a smooth muscle cell-like phenotype (myofibroblast) to aid in remodeling and contraction of wound sites [34, 35]. Myofibroblasts are also associated with numerous pathological conditions, such as fibrous scarring, aortic valve calcification, and other fibrotic diseases, usually when environmental variables result in an over-abundance of myofibroblasts [34, 36]. Fibroblasts express basal levels of αSMA, however, increased αSMA expression and formation of αSMA stress fibers is indicative of myofibroblast phenotype [34, 35, 37]. There are several known modulators of myofibroblast phenotype, the most notable are stimulation with transforming growth factor β1 (TGF- β1), and mechanical forces arising from dynamically changing strain and substrate stiffness [35, 36, 38, 39]. Furthermore, αSMA expression has been shown to correlate with fibroblast contractile ability, and is upregulated on stiffer substrates, and can be dynamically modulated by changing substrate stiffness [35, 39, 40]. In the present study, we investigated the cellular response to patterned SiO_2 substrates in the context of αSMA expression to determine if needles altered the contractility or myofibroblasts phenotype of 3T3 fibroblasts. Neo-expression of αSMA was not observed on any of the test substrates, αSMA expression was not significantly different, and αSMA stress fibers were not evident in fibroblasts cultured on either substrate (Figure 4B-C). This indicates that culture of 3T3 fibroblasts on SiO_2 substrates does not induce a myofibroblast phenotype. However, fibroblasts which formed large clumps on flat substrates were not analyzed for αSMA expression. These clumps of cells demonstrate similar morphology to fibroblasts which form calcific nodules in aortic valve disease [40, 41]. Because these test substrates have a high surface modulus, which has been shown to induce myofibroblast formation, we would expect to see the contraction of fibroblasts into nodules when seeded on SiO_2 substrates. Clump formation was significantly lower on patterned nanoneedles substrates, which suggests that interrupting cell-cell interactions in favor of cell-matrix interactions decreases the contractile ability of fibroblasts, even when seeded on stiff substrates.

The utility of this surface format for basic and applied biological sciences and biomedical engineering lies in its ability to manipulate cell behavior in order to probe fundamental biological processes and pathological mechanisms. This technique is versatile and other materials, such as synthetic polymers, can be used in the place of CA through a simple solvent casting approach. Material properties (i.e. stiffness, hydrophobicity/philicity, charge) impact cell health and fate, and can be tuned through copolymerization [42, 43]. For example, our laboratory has used copolymers with subunits of varying molar ratios to alter material properties and control cell health, proliferation, and differentiation [42, 43]. By applying these polymers in the nanoneedle format, we plan to use synthetic surfaces to

investigate tissue formation/regeneration and early mechanisms in cancerous transformation of human cells.

3. Conclusions

Single-pulse femtosecond laser machined templates were used to extract gradient patterns of CA nanoneedles by replication. After coating CA nanoneedles with silica, the resulting 3D silica nanoneedle patterns were used to study the effect of two dimensional gradient spacing on cell-cell and cell-matrix interactions that play a mechanistic role in tissue regeneration as well as pathogenesis. The technique is useful in understanding cell biology with possible application to the study of cell lineage transition, particularly the mesenchymal-to-epithelial transition and myofibroblast phenotype expression. The advantage of this process is the ease and control of geometrical structuring by femtosecond laser machining. We foresee the use of this technology and advanced polymers to engineer synthetic surfaces for tissue regeneration.

Acknowledgments

The Tennessee Higher Education Commission supported this work through a grant to the Center for Laser Applications, University of Tennessee Space Institute. We also would like to acknowledge support from the National Institutes of Health (NIH HL091465) and the National Science Foundation (CAREER: CBET 1056046). This work was also supported by the Vanderbilt Institute of Nanoscale Science and Engineering (VINSE).

REFERNCES

1. Geiger B, Spatz JP, Bershadsky AD. Environmental sensing through focal adhesions. Nat Rev Mol Cell Biol. 2009; 10:21–33. [PubMed: 19197329]
2. Hoffman-Kim, D.; Mitchel, JA.; Bellamkonda, RV. Topography, Cell Response, and Nerve Regeneration. In: Yarmush, ML.; Duncan, JS.; Gray, ML., editors. Annual Review of Biomedical Engineering. Vol. 12. Annual Reviews; Palo Alto: 2010. p. 203-231.
3. Bettinger CJ, Langer R, Borenstein JT. Engineering Substrate Topography at the Micro- and Nanoscale to Control Cell Function. Angewandte Chemie International Edition. 2009; 48:5406–5415.
4. Chandra P, Lai K, Sung HJ, Murthy NS, Kohn J. UV laser-ablated surface textures as potential regulator of cellular response. Biointerphases. 2010; 5:53–59. [PubMed: 20831349]
5. Ross AM, Jiang ZX, Bastmeyer M, Lahann J. Physical Aspects of Cell Culture Substrates: Topography, Roughness, and Elasticity. Small. 2012; 8:336–355. [PubMed: 22162324]
6. Stevens MM, George JH. Exploring and Engineering the Cell Surface Interface. Science. 2005; 310:1135–1138. [PubMed: 16293749]
7. Harrison RG. The cultivation of tissues in extraneous media as a method of morphogenetic study. Anatomical Record. 1912; 6:181–193.
8. Harrison RG. The reaction of embryonic cells to solid structures. Journal of Experimental Zoology. 1914; 17:521–544.
9. Alves NM, Pashkuleva I, Reis RL, Mano JF. Controlling Cell Behavior Through the Design of Polymer Surfaces. Small. 2010; 6:2208–2220. [PubMed: 20848593]
10. Curtis A, Wilkinson C. Topographical control of cells. Biomaterials. 1997; 18:1573–1583. [PubMed: 9613804]
11. Ekblom P, Vestweber D, Kemler R. Cell-matrix interactions and cell adhesion during development. Annu Rev Cell Biol. 1986; 2:27–47. [PubMed: 3548769]
12. Lord MS, Foss M, Besenbacher F. Influence of nanoscale surface topography on protein adsorption and cellular response. Nano Today. 2010; 5:66–78.
13. Singhvi R, Stephanopoulos G, Wang DIC. Effects of substratum morphology on cell physiology. Biotechnology and Bioengineering. 1994; 43:764–771. [PubMed: 18615800]

14. Curtis ASG, Varde M. Control of Cell Behavior - Topological Factors. Journal of the National Cancer Institute. 1964; 33:15. [PubMed: 14202300]
15. Dunn GA, Heath JP. New Hypothesis of Contact Guidance in Tissue-Cells. Experimental Cell Research. 1976; 101:1–14. [PubMed: 182511]
16. Ohara PT, Buck RC. Contact guidance in vitro: A light, transmission, and scanning electron microscopic study. Experimental Cell Research. 1979; 121:235–249. [PubMed: 571804]
17. Weiss P. Experiments on cell and axon orientation in vitro: The role of colloidal exudates in tissue organization. Journal of Experimental Zoology. 1945; 100:353–386. [PubMed: 21010856]
18. Clark P, Connolly P, Curtis ASG, Dow JAT, Wilkinson CDW. Topographical Control of Cell Behavior 1. Simple Step Cues. Development. 1987; 99:439–448. [PubMed: 3653011]
19. Clark P, Connolly P, Curtis ASG, Dow JAT, Wilkinson CDW. Topographical Control of Cell Behavior 2. Multiple Grooved Substrata. Development. 1990; 108:635–644. [PubMed: 2387239]
20. Norman J, Desai T. Methods for fabrication of nanoscale topography for tissue engineering scaffolds. Annals of Biomedical Engineering. 2006; 34:89–101. [PubMed: 16525765]
21. Choi C-H, Hagvall SH, Wu BM, Dunn JCY, Beygui RE, Kim C-J-Cj. Cell interaction with three-dimensional sharp-tip nanotopography. Biomaterials. 2007; 28:1672–1679. [PubMed: 17174392]
22. Ghibaudo M, Di Meglio JM, Hersen P, Ladoux B. Mechanics of cell spreading within 3D-micropatterned environments. Lab on a Chip. 2011; 11:805–812. [PubMed: 21132213]
23. Ghibaudo M, Trichet L, Le Digabel J, Richert A, Hersen P, Ladoux B. Substrate Topography Induces a Crossover from 2D to 3D Behavior in Fibroblast Migration. Biophysical Journal. 2009; 97:357–368. [PubMed: 19580774]
24. Green AM, Jansen JA, van der Waerden JPCM, Von Recum AF. Fibroblast response to microtextured silicone surfaces: Texture orientation into or out of the surface. Journal of Biomedical Materials Research. 1994; 28:647–653. [PubMed: 8027105]
25. Su WT, Liao YF, Lin CY, Li LT. Micropillar substrate influences the cellular attachment and laminin expression. Journal of Biomedical Materials Research Part A. 2010; 93A:1463–1469. [PubMed: 19967757]
26. Biname F, Pawlak G, Roux P, Hibner U. What makes cells move: requirements and obstacles for spontaneous cell motility. Molecular BioSystems. 2010; 6:648–661. [PubMed: 20237642]
27. Ng C, Yu K. Proliferation of Epithelial Cells on PDMS Substrates with Micropillars Fabricated with Different Curvature Characteristics. Biointerphases. 2012; 7:1–8. [PubMed: 22589044]
28. Sung HJ, Su J, Berglund JD, Russ BV, Meredith JC, Galis ZS. The use of temperature composition combinatorial libraries to study the effects of biodegradable polymer blend surfaces on vascular cells. Biomaterials. 2005; 26:4557–4567. [PubMed: 15722125]
29. Rajput D, Costa L, Terekhov A, Lansford K, Hofmeister W. Silica coating of polymer nanowires produced via nanoimprint lithography from femtosecond laser machined templates. Nanotechnology. 2012; 23:105304. [PubMed: 22361985]
30. Zalloum OHY, Parrish M, Terekhov A, Hofmeister W. An amplified femtosecond laser system for material micro-/nanostructuring with an integrated Raman microscope. Review of Scientific Instruments. 2010; 81:053906–053907. [PubMed: 20515154]
31. Zalloum OHY, Parrish M, Terekhov A, Hofmeister W. On femtosecond micromachining of HPHT single-crystal diamond with direct laser writing using tight focusing. Opt Express. 2010; 18:13122–13135. [PubMed: 20588442]
32. Lutolf MP, Hubbell JA. Synthetic biomaterials as instructive extracellular microenvironments for morphogenesis in tissue engineering. Nat Biotechnol. 2005; 23:47–55. [PubMed: 15637621]
33. Thompson EW, Newgreen DF, Tarin D. Carcinoma invasion and metastasis: a role for epithelial-mesenchymal transition? Cancer Res. 2005; 65:5991–5995. discussion 5995. [PubMed: 16024595]
34. Desmouliere A, Chaponnier C, Gabbiani G. Tissue repair, contraction, and the myofibroblast. Wound repair and regeneration : official publication of the Wound Healing Society [and] the European Tissue Repair Society. 2005; 13:7–12.
35. Hinz B, Celetta G, Tomasek JJ, Gabbiani G, Chaponnier C. Alpha-smooth muscle actin expression upregulates fibroblast contractile activity. Molecular Biology of the Cell. 2001; 12:2730–2741. [PubMed: 11553712]

36. Gabbiani G. The myofibroblast in wound healing and fibrocontractive diseases. Journal of Pathology. 2003; 200:500–503. [PubMed: 12845617]

37. Leavitt J, Gunning P, Kedes L, Jariwalla R. Smooth-Muscle Alpha-Actin Is a Transformation-Sensitive Marker for Mouse Nih 3t3 and Rat-2 Cells. Nature. 1985; 316:840–842. [PubMed: 4033781]

38. Kloxin AM, Benton JA, Anseth KS. In situ elasticity modulation with dynamic substrates to direct cell phenotype. Biomaterials. 2010; 31:1–8. [PubMed: 19788947]

39. Yip CYY, Chen JH, Zhao RG, Simmons CA. Calcification by Valve Interstitial Cells Is Regulated by the Stiffness of the Extracellular Matrix. Arteriosclerosis Thrombosis and Vascular Biology. 2009; 29:936–U417.

40. Benton JA, Kern HB, Anseth KS. Substrate Properties Influence Calcification in Valvular Interstitial Cell Culture. Journal of Heart Valve Disease. 2008; 17:689–699. [PubMed: 19137803]

41. Chen JH, Yip CYY, Sone ED, Simmons CA. Identification and Characterization of Aortic Valve Mesenchymal Progenitor Cells with Robust Osteogenic Calcification Potential. American Journal of Pathology. 2009; 174:1109–1119. [PubMed: 19218344]

42. Crowder SW, Gupta MK, Hofmeister LH, Zachman AL, Sung HJ. Modular polymer design to regulate phenotype and oxidative response of human coronary artery cells for potential stent coating applications. Acta Biomaterialia. 2012; 8:559–569. [PubMed: 22019760]

43. Gupta MK, Walthall JM, Venkataraman R, Crowder SW, Jung DK, Yu SS, Feaster TK, Wang X, Giorgio TD, Hong CC, Baudenbacher FJ, Hatzopoulos AK, Sung HJ. Combinatorial Polymer Electrospun Matrices Promote Physiologically-Relevant Cardiomyogenic Stem Cell Differentiation. PLoS One. 2011; 6:e28935. [PubMed: 22216144]

Highlights

- Tunable geometry of nanoneedle patterns affects cell-cell, cell-matrix interactions.
- 3D silica nanostructure substrates are reproducible by nanoimprinting and coating.
- Patterned substrates are easily fabricated from reusable templates.
- Direct write process enables reproduction of any pattern geometry.

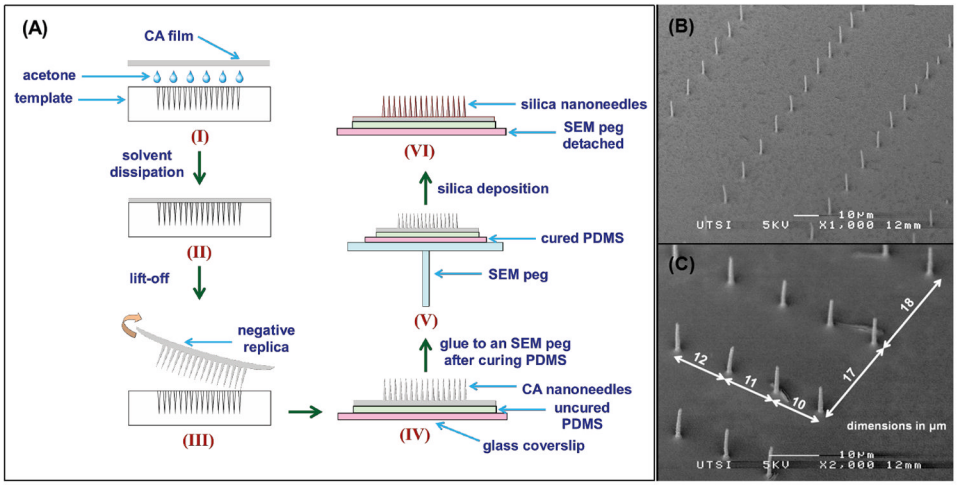

Figure 1. Pattern prepared on fused silica substrate by single-pulse femtosecond laser machining

(A) A schematic of the pattern displaying the 2D gradient in nanohole spacing (nanohole density reduced for visual clarity). The pattern is a 2×2 matrix of four quadrants, each formed by increasing the spacing between successive nanoholes by 1 μm starting from 10 μm in the densest location (edge) to 50 μm in the sparsest location (middle of the quadrant) and then decreasing from 50 μm to 10 μm at 1 μm decrements in both x and y directions. A quadrant is a matrix of 84×84 nanoholes, and a 2×2 matrix of these quadrants forms the pattern with 168×168 nanoholes. Each black dot in the schematic represents a nanohole made by focusing a single laser pulse. **(B)** An SEM image of the nanoholes from one edge of the pattern.

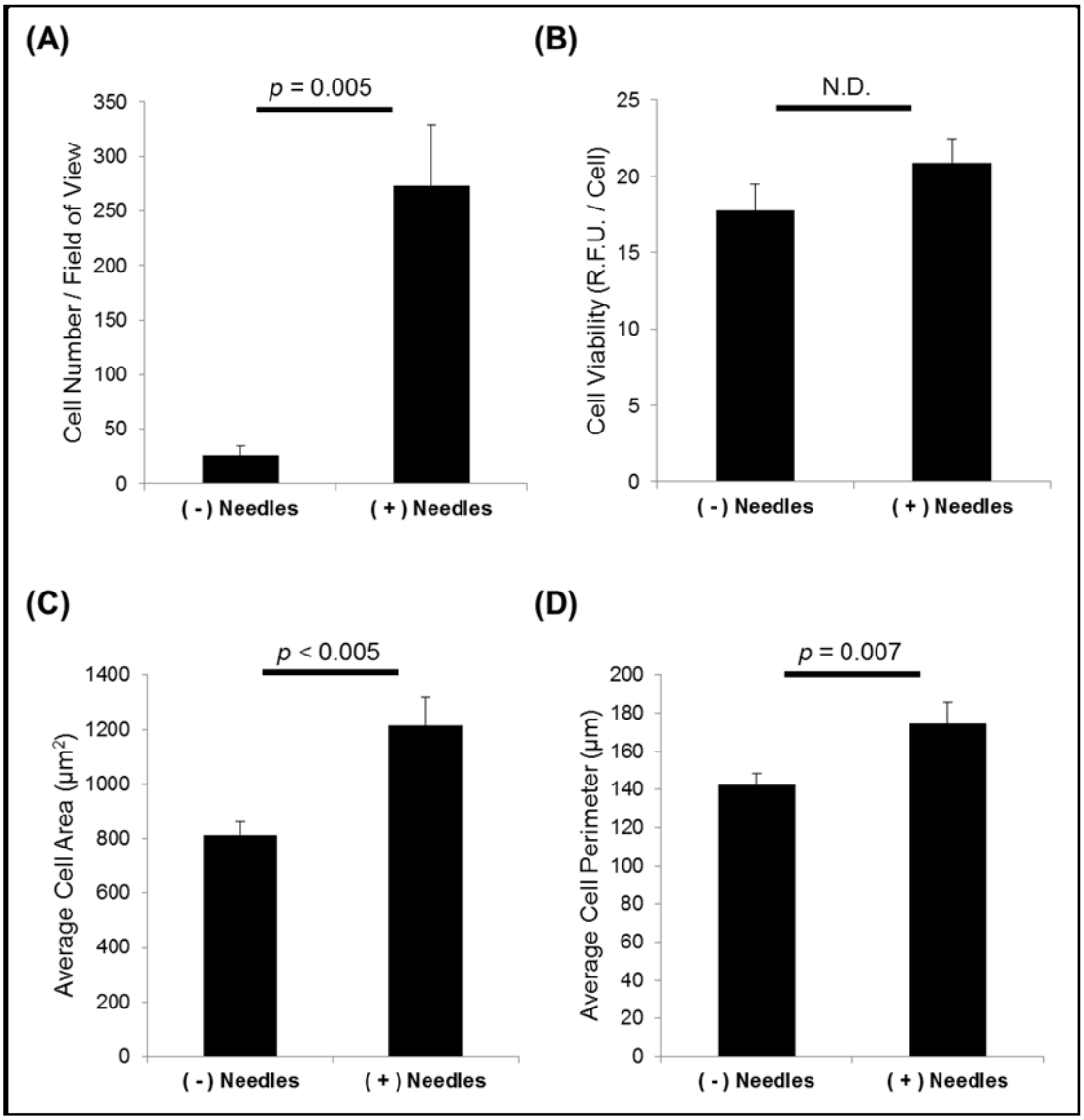

Figure 2. Silica nanoneedle fabrication

(A) Schematic of the fabrication of silica nanoneedles starting from cellulose acetate (CA) replication of the laser patterned fused silica template (steps I and II). The replica with CA nanoneedles is then peeled off from the template and glued to a 170 μm glass coverslip with uncured PDMS, and cured at room temperature for 24 hours (steps III and IV). The glass coverslip with CA nanoneedles is then affixed to an aluminum SEM peg (step V) and subjected to silica deposition to form silica nanoneedles. The glass coverslip with silica nanoneedles is then detached from the SEM peg by selectively dissolving the sticky tab adhesive in toluene. **(B)** SEM image of silica pattern in a specific location where nanoneedles are densely spaced in one direction and sparsely spaced in the orthogonal direction. **(C)** SEM images of silica nanoneedles (taken at 45° stage tilt) from a section of the 2D gradient pattern at one edge illustrating the x and y increment of 1 μm every successive nanohole.

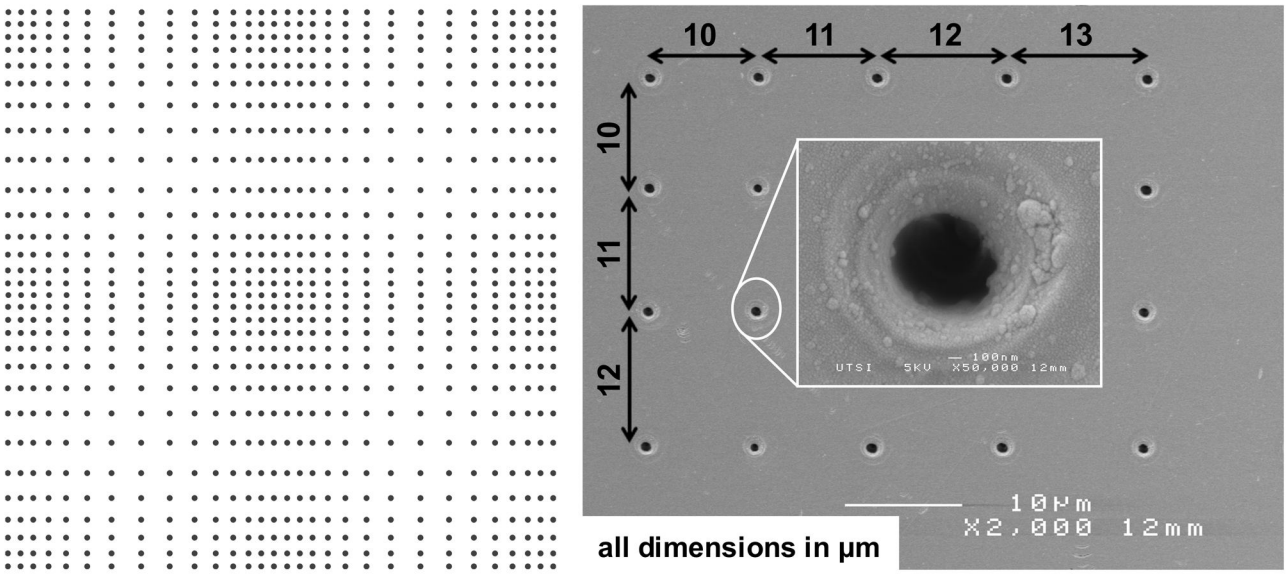

Figure 3. SiO_2 nanoneedles promote cell attachment and spreading

(A) Significantly more cells attach to nanoneedle-containing surfaces and **(B)** cell viability is unaffected. **(C–D)** Cell spreading (area, perimeter) are increased on nanoneedle-containing substrates.

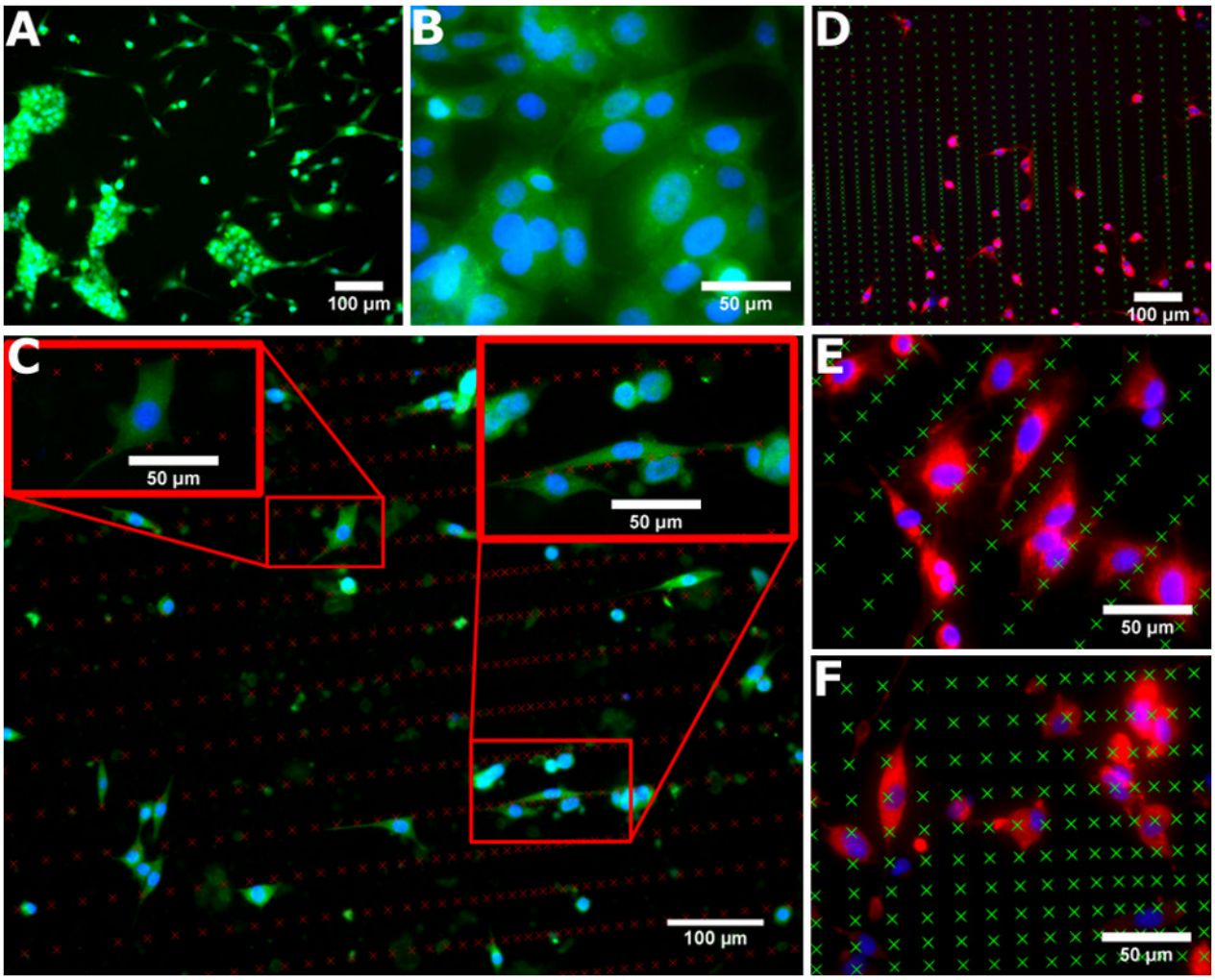

Figure 4. Cell adhesion is influenced by the presence and spacing of SiO_2 nanoneedles

(A–B) Flat surfaces promote the formation of large, unorganized cell aggregates. **(C–D)** Cells interact directly with the nanoneedles and only small cell aggregates, if any, are able to form. **(E)** Parallel rows of tightly spaced nanoneedles sequester cells between them. **(F)** Few, if any, cells are able to attach in areas of densely packed nanoneedles, but attachment improves as spacing becomes sparser. Nanoneedle locations are indicated by X's in each image. **A:** calcein, green; **B–C:** αSMA, green; Hoechst, blue; **D–F:** actin, red; Hoechst, blue.